Permeability Control by Cholinergic Receptors in *Torpedo* Postsynaptic Membranes: Agonist Dose–Response Relations Measured at Second and Millisecond Times†

Richard R. Neubig and Jonathan B. Cohen*

ABSTRACT: A quantitative analysis of nicotinic acetylcholine receptor function in *Torpedo* postsynaptic membranes is presented. $^{22}Na^+$ efflux induced by carbamylcholine (Carb) and the partial agonist phenyltrimethylammonium (PTA) is assessed by determining dose–response relations using three approaches: (1) a filtration assay measuring responses on the 10-s time scale, (2) the same filtration assay after blocking different fractions of the receptor sites with α-bungarotoxin (α-BgTx), and (3) a rapid-mix quenched-flow technique which permits measurement of the initial rate of $^{22}Na^+$ efflux on the millisecond time scale. The concentrations of agonist producing half-maximal responses in these three assays at 4 °C are 13, 150, and 600 μM, respectively, for Carb and 50, 50, and 200 μM, respectively, for PTA. The rate constants for $^{22}Na^+$ efflux are 1.3×10^{-4} s^{-1} in the absence of agonist and 65 s^{-1} and 0.8 s^{-1} in the presence of maximal concentrations of Carb and PTA, respectively, representing a stimulation of 5×10^5 by Carb. The Hill coefficient for the Carb response, expressed as rate constants for $^{22}Na^+$ efflux, is 1.97 ± 0.06 for Carb concentrations between 3 μM and 1 mM. The inhibition of the agonist-stimulated $^{22}Na^+$ efflux by α-BgTx is compatible with two α-BgTx (and acetylcholine) sites per functional unit. Inhibition of Carb responses (slow assay) by *d*-tubocurarine appears competitive with a $K_I \sim 0.5$ μM, while responses to PTA are inhibited noncompetitively with K_I = 0.3 μM. This paradox is due to the presence of spare receptors and to complexities in the binding of dTC to the nicotinic acetylcholine receptor. Determination of responses without the complication of spare receptors allows a meaningful comparison to direct measurements of agonist and antagonist binding in the same system. A model is proposed to account for both binding and response.

The binding of acetylcholine (AcCh)[1] by nicotinic cholinergic receptors results in the formation of cation-selective transmembrane channels. These channels are only open transiently, since the equilibrium binding of cholinergic agonists is not associated with enhanced membrane permeability. Rather, desensitization occurs (Katz & Thesleff, 1957). To understand how the energetics of agonist binding result in channel activation and desensitization, it is necessary to characterize under identical conditions both the conformational equilibria of the receptor defined by ligand binding and the functional state of the ion channel. Electrophysiological studies provide extensive information about the permeability response without providing direct information about the kinetics of ligand binding [for a review, see Gage (1976)].

Nicotinic postsynaptic membranes isolated from *Torpedo* electric organs (Cohen et al., 1972) provide a unique preparation for the analysis of the mechanism of permeability control by the nicotinic cholinergic receptor [for a review, see Heidmann & Changeux (1978)]. Membrane suspensions containing micromolar concentrations of receptor binding sites are readily attainable. This permits detailed analysis of the equilibrium binding and the kinetics of binding of cholinergic agonists (Heidmann & Changeux, 1979; Weiland et al., 1977; Quast et al., 1978; Cohen & Boyd, 1979), competitive antagonists (Neubig & Cohen, 1979), and also noncompetitive antagonists such as histrionicotoxin (Eldefrawi et al., 1978; Elliot & Raftery, 1979) and meproadifen (Krodel et al., 1979; Neubig et al., 1979). In addition, since Kasai & Changeux (1971) introduced a filtration assay to measure the agonist-stimulated efflux of ions from vesicles isolated from *Electrophorus* electric tissue, the experimental basis for measuring cholinergic permeability responses in isolated vesicles has been available.

In previous experiments, ion fluxes from *Torpedo* vesicles could be measured only at times greater than 10 s after addition of agonist (Popot et al., 1976; Andreasen & McNamee, 1977; Miller et al., 1978; Neubig et al., 1979). Flux responses determined on this time scale do not provide a direct measure of receptor activation because of the high density of nicotinic receptors in those membranes ($\sim 10\,000/\mu m^2$; Cartaud et al., 1973). At 0.1 mM carbamylcholine (Carb), the $^{22}Na^+$ within the vesicles is fully released by the first measurements. This phenomenon, in which only a small fraction of the available receptors need be activated to generate the maximum observable response, can be characterized as one of "spare" receptors (Stephenson, 1956), and in this case agonist concentrations producing half-maximal responses are not directly related to receptor affinities.

Two approaches can be utilized to circumvent the problem of spare receptors. First, one can inactivate a fraction of the receptors with an irreversible antagonist (Furchgott, 1966; Furchgott & Bursztyn, 1967). At a sufficient degree of receptor inactivation, the response measured after several seconds or minutes should be proportional to the number of receptors activated by agonist. Second, and more directly, the response can be measured at appropriately short times to determine the initial rate of release of $^{22}Na^+$ for different agonist concentrations. To do this, it is necessary to mix membrane suspensions with agonist and to terminate the agonist-induced efflux on a millisecond time scale. Rapid-mixing techniques in conjunction with a spectrometric detection system have been

† From the Department of Pharmacology, Harvard Medical School, Boston, Massachusetts 02115. *Received January 2, 1980.* This research was supported by U.S. Public Health Service Grant NS 12408 and by a grant from the Sloan Foundation. R.R.N. is supported by U.S. Public Health Service Predoctoral Training Grant GM 07753, and J.B.C. is a recipient of U.S. Public Health Service Research Scientist Career Development Award NS 01555.

[1] Abbreviations used: AcCh, acetylcholine; α-BgTx, α-bungarotoxin; dTC, *d*-tubocurarine; meproadifen, 2-[(diethylmethyl)amino]ethyl-2,2-diphenylvalerate; TPS, *Torpedo* physiological saline (250 mM NaCl, 5 mM KCl, 3 mM $CaCl_2$, 2 mM $MgCl_2$, and 5 mM NaP_i, pH 7).

0006-2960/80/0419-2770$01.00/0

used to monitor a variety of biochemical events [for a review, see Chance (1974)]. Rapid mixing can be used in the absence of a spectroscopic signal if the reaction can be stopped (quenched) by a chemical means such as a pH change (Barman & Gutfreund, 1964) or substrate chelation. The extent of the reaction at the time it was stopped can then be determined on a slower more convenient time scale. With appropriate quench solutions, phosphorylation of sarcoplasmic reticulum vesicles and the transport of Ca^{2+} into those vesicles have been measured on the millisecond time scale (Froehlich & Taylor, 1976; Sumida et al., 1978).

We report here analyses of the agonist-stimulated efflux of $^{22}Na^+$ from *Torpedo* vesicles using both approaches outlined above. Dose–response relations were determined (1) after relatively long exposure to agonist (20 s) under conditions where known amounts of the cholinergic receptor binding sites are occupied by α-bungarotoxin (α-BgTx) and (2) by a rapid-mix quenched-flow technique that permits the direct analysis of the rate of efflux of $^{22}Na^+$ on the millisecond time scale. The reaction was quenched with cholinergic antagonists, and efflux was assayed by ultrafiltration. Dose–response relations determined by the two methods are comparable, and the results obtained are discussed in terms of current knowledge of the binding of cholinergic agonists and antagonists by the *Torpedo* vesicles.

Materials and Methods

AcCh Receptor-Rich Membranes. Acetylcholine (AcCh) receptor-rich membranes were prepared from freshly dissected *Torpedo californica* and *Torpedo nobiliana* electric organs as described by Sobel et al. (1977). Membrane suspensions were stored at 4 °C in 37% (w/w) sucrose–0.02% NaN_3. The binding of ^3H-labeled *Naja nigricollis* α-toxin was measured as described (Neubig & Cohen, 1979), and membrane protein concentration was determined by the method of Lowry et al. (1951). Specific activities (in micromoles of α-toxin sites per gram of protein) were 1.2–1.9 for *T. californica* (five fish) and 2.2 for *T. nobiliana* (one fish). No differences were observed between those of two species in $^{22}Na^+$ efflux experiments.

Measurements of $^{22}Na^+$ Efflux. The efflux of $^{22}Na^+$ from *Torpedo* vesicles was measured at 4 °C by a filtration assay that is a modification of the procedure of Neubig et al. (1979). Concentrated membrane suspensions were incubated overnight at 4 °C with 40 μCi of $^{22}Na^+$ per mL in *Torpedo* physiological saline (TPS): 250 mM NaCl, 5 mM KCl, 3 mM $CaCl_2$, 2 mM $MgCl_2$, and 5 mM NaP_i, pH 7.0. This suspension was passed over a 3-mL Dowex 50-W ion-exchange column and then diluted with TPS to initiate an efflux experiment. The ion-exchange column removes ~90% of the external $^{22}Na^+$, which decreases the filter background and also reduces radiation exposure. Diluted membrane suspensions were usually allowed to equilibriate for 20 min before characterization of agonist-stimulated efflux to permit release of $^{22}Na^+$ from poorly sealed vesicles (Hess & Andrews, 1977; Eldefrawi et al., 1978). $^{22}Na^+$ retention within the vesicles was determined by filtration of 1-mL aliquots on glass fiber (Whatman GF/F) filters followed by a rapid wash with 10 mL of TPS. Filters were prerinsed with 2 mL of TPS.

Agonist-stimulated efflux was determined by two different procedures. (1) For characterization of $^{22}Na^+$ retention at times greater than 10 s after addition of agonist, a small volume of concentrated solution containing agonist was added to the diluted suspension, the mixture was agitated, and aliquots were filtered at desired intervals. Results reported here are primarily concerned with the characterization of agonist dose–response relations determined at a fixed time (20 s) after addition of agonist. (2) The rate of $^{22}Na^+$ efflux at subsecond times was determined by quenched-flow techniques.

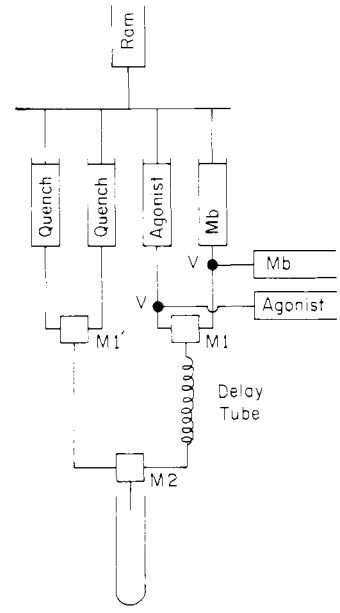

FIGURE 1: Schematic diagram of quench-flow apparatus. Four syringes are driven simultaneously by a pneumatic ram. The membranes (Mb) and agonist are mixed in an eight-jet tangential mixer (M1; Durrum Instruments, Palo Alto, CA), and after passing through the Teflon delay tube the reaction is quenched in a second eight-jet mixer (M2). The reaction time is altered by varying the volume of the delay tube or the velocity of fluid flow. The solid circles (V) represent manual four-way valves which allow filling of the reactant syringes from reservoir syringes and washing of the delay tube before the next run.

The fraction of $^{22}Na^+$ released from the vesicles 20 s after addition of agonist was determined as follows (see also Figure 2). Aliquots of the diluted suspension were filtered between 20 and 100 min after passage over the ion-exchange column to establish the unstimulated efflux of $^{22}Na^+$ from the *Torpedo* vesicles. Drug solutions were added to other aliquots which were shaken and filtered 20 s later. There was no significant $^{22}Na^+$ leakage induced by shaking, as determined by control samples which received drug diluent only. The response was expressed as the percent of $^{22}Na^+$ retained on the filter relative to that retained at that time after dilution in the absence of drug (i.e., unstimulated efflux). A filter blank, consisting of the $^{22}Na^+$ retained in the absence of any vesicles (100–200 cpm), was subtracted from all data. When agonist-stimulated $^{22}Na^+$ efflux was to be determined for vesicles with receptors partially blocked by α-neurotoxin, membrane suspensions were incubated with α-BgTx during the overnight equilibration with $^{22}Na^+$ and the extent of blockage was determined by measuring the binding of ^3H-labeled *N. nigricollis* α-toxin. In experiments with *d*-tubocurarine (dTC), the membrane suspensions were preincubated for 15 min with dTC before the addition of agonist.

Quenched-Flow Determination of $^{22}Na^+$ Efflux. Agonist-stimulated efflux of $^{22}Na^+$ from dilute membrane suspensions was measured on the millisecond time scale by the use of a four-syringe quenched-flow apparatus (Figure 1). Activation of a pneumatic ram results in the rapid mixing (mixer 1) of equal volumes of the membrane suspension containing $^{22}Na^+$ with a TPS solution containing agonist. That mixture then flows through a delay tube to a second mixer (mixer 2) in which it is mixed with a quench solution containing 2 mM dTC and 0.2 mM meproadifen (a noncompetitive antagonist) in TPS. $^{22}Na^+$ retained within the vesicles was then deter-

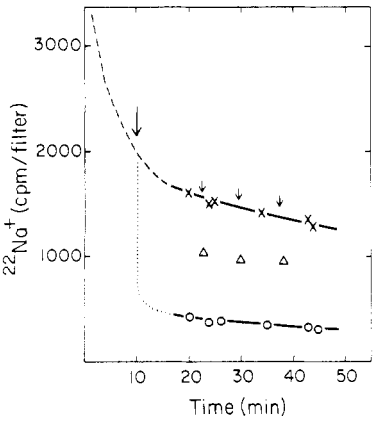

FIGURE 2: $^{22}Na^+$ efflux from *T. californica* membrane vesicles. Membranes (2.4 mg of protein) were incubated overnight in 0.3 mL of TPS containing 40 μCi/mL $^{22}Na^+$ and then loaded on a 3-mL Dowex 50-W column, eluted with 3 mL of TPS, and diluted to 45 mL. Samples (1 mL) were filtered to determine the passive efflux curve (×); 0.1 mM Carb was added (large arrow) to 7 mL of the diluted membranes, and 1-mL aliquots were filtered (○) to determine the maximum amount of $^{22}Na^+$ releasable by this agonist. Addition of 10 μM Carb with shaking (small arrows) followed 20 s later by filtration (△) constitutes the determination of one point of a dose–response curve. The entire control dose–response curve (× in Figure 4A) was produced similarly during this 50-min experiment. The dashed line indicates the early time course of passive $^{22}Na^+$ efflux determined in previous experiments, and the dotted line indicates efflux induced by 0.1 mM Carb. The filter blank (200 cpm) has not been subtracted from these data.

mined by filtration. The duration of exposure of the membranes to agonist alone was varied from 24 to 550 ms by varying the air pressure driving the ram or the length of the delay tube between mixers 1 and 2. Eight-jet tangential mixers (Gibson & Milnes, 1964) were utilized, and the apparatus was calibrated by measuring the hydrolysis of *o*-nitrophenylacetate by 1 M NaOH with 1 M HCl as a quench solution. Rate constants (k_{OH}) for hydroxide ion catalyzed hydrolysis of this ester at 4 °C (k_{OH} = 1.4 M^{-1} s^{-1}) and 22 °C (k_{OH} = 12 M^{-1} s^{-1}) determined in this apparatus agreed well with published values: k_{OH} = 25 M^{-1} s^{-1} at 30 °C (Holmquist & Bruice, 1969).

Rate constants for $^{22}Na^+$ efflux measured by the quenched-flow technique were determined by linear least-squares analysis of semilogarithmic plots of $F_\infty - F_t$ against t, where F_∞ is the fraction of $^{22}Na^+$ released after exposure to agonist for several minutes and F_t is the fraction released after time t. Analysis of $^{22}Na^+$ efflux for low agonist concentrations (Figure 3) required a different method. Desensitization occurred on the second time scale as reflected in the nonlinear semilogarithmic plots of $F_\infty - F_t$ against t (plots not shown). Consequently, initial rates of efflux were determined by fitting F_t vs. t to the equation

$$F_t = F_{max}\{1 - \exp[-(k_o/k_d)[1 - \exp(-k_d t)]]\}$$

with a nonlinear least-squares program (Bard, 1967). F_{max} represents the maximal fraction of $^{22}Na^+$ released by high agonist concentrations, and k_o and k_d are rate constants for $^{22}Na^+$ efflux and the appearance of desensitization, respectively, for the Carb concentration being studied. This expression can be derived by integration of eq 9 and 16 of Bernhardt & Neumann (1978).

Results

Characterization of $^{22}Na^+$ Efflux from Torpedo Vesicles. The unstimulated efflux of $^{22}Na^+$ from *Torpedo* receptor-rich membrane vesicles cannot be characterized by a single rate

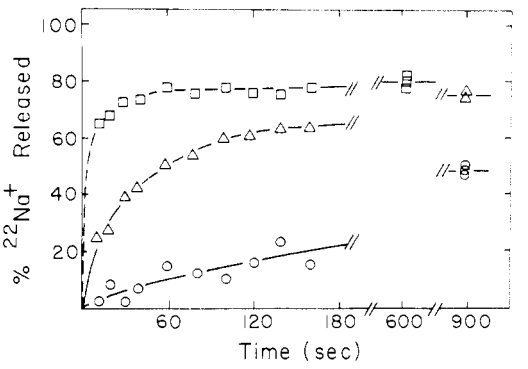

FIGURE 3: Kinetics of $^{22}Na^+$ efflux at low Carb concentrations (4 °C). A suspension of *T. californica* vesicles containing 20 μM α-BgTx sites was incubated overnight at 4 °C in TPS with 40 μCi/mL $^{22}Na^+$. The membranes were diluted to 150 nM α-BgTx sites after passage over a Dowex 50-W column. These $^{22}Na^+$-loaded membranes were mixed by using syringes and a "T" mixer with equal volumes of TPS containing Carb to give final concentrations of 3 (○), 10 (△), and 30 (□) μM. Aliquots (1 mL) were filtered at the indicated times to determine the amount of $^{22}Na^+$ retained in the vesicles. The fraction of $^{22}Na^+$ released was calculated as described under Materials and Methods.

constant. However, a significant portion of the $^{22}Na^+$ is contained within a population of well sealed vesicles characterized by half-times of release in excess of 60 min (Figure 2). In typical preparations, the retained volume 30 min after passage over the ion-exchange column was ~50% of that determined within 30 s after passage over the column.

The vesicles sealed to $^{22}Na^+$ are characterized by two parameters: an internal volume (microliters of solution per milligram of protein) and the fraction of that volume equilibrated rapidly upon exposure to high concentrations of cholinergic agonist. In a typical experiment shown in Figure 2, the $^{22}Na^+$ retained 20 min after passage over the ion-exchange column was equivalent to an internal volume of 0.31 μL/mg of protein and ~75% of that volume was equilibrated upon exposure to 0.1 mM Carb. Higher concentrations of Carb did not cause greater release of $^{22}Na^+$. The maximal fraction of $^{22}Na^+$ released by Carb is correlated with the purity of the membrane suspensions, ranging from 10% for membranes containing 0.1 μmol of α-toxin sites per g of protein to greater than 90% for membrane suspensions containing 3 μmol of α-toxin sites per g of protein. Thus, it appears that the internal volume not responsive to Carb is probably associated with vesicles containing no functional receptor. That the $^{22}Na^+$ is retained within sealed vesicles is evidenced by the fact that it is released by addition of gramicidin (15 μg/mL).

Agonist-Stimulated Efflux of $^{22}Na^+$. Exposure of *Torpedo* membranes to 100 μM Carb results in a complete equilibration of $^{22}Na^+$ in less than 10 s (Neubig et al., 1979; Miller et al., 1978). $^{22}Na^+$ efflux following addition of 30 μM Carb or less can be characterized by an assay with a resolution of 10 s (Figure 3). The initial rate of efflux of $^{22}Na^+$ in the presence of 3 and 10 μM Carb represents a 12- and 110-fold enhancement over the unstimulated efflux rate. This stimulated efflux is transient; after 15 min in the presence of 3 μM Carb, the efflux rate is essentially that of unstimulated efflux and only 60% of the internal $^{22}Na^+$ was released by that time. This loss of responsiveness to agonist, known as desensitization (Katz & Thesleff, 1957), has been described for membrane suspensions isolated from *Torpedo marmorata* (Sugiyama et al., 1976; Bernhardt & Neuman, 1978), and we report elsewhere a quantitative analysis of the kinetics of densensitization (R. R. Neubig and J. B. Cohen, unpublished results). At this point we wish to define agonist dose–response relations based

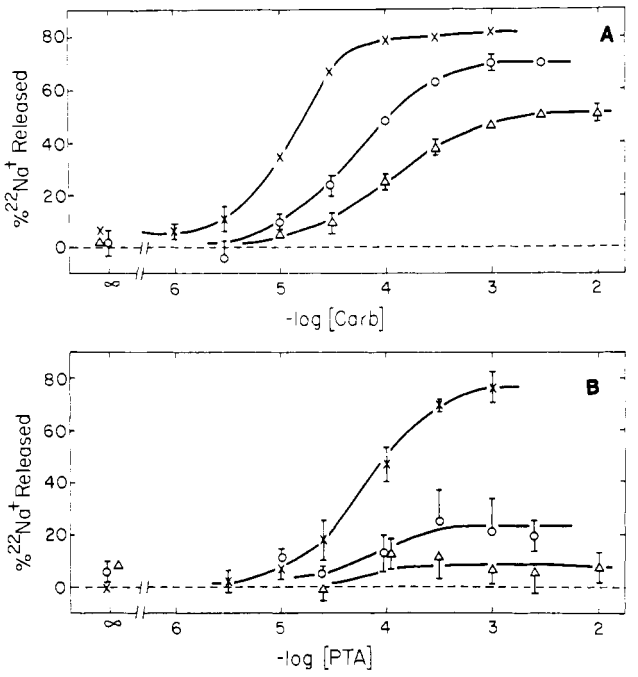

FIGURE 4: $^{22}Na^+$ release by Carb and PTA from *T. californica* membranes partially blocked with α-BgTx. Dose–response relations at 4 °C for $^{22}Na^+$ released 20 s after addition of agonists were determined as described in the legend to Figure 2 and under Materials and Methods. (A) Carb responses when 0 (×), 47 (○), or 73% (△) of the nicotinic receptor sites are occupied by α-BgTx. (B) Dose–response relations for PTA-induced $^{22}Na^+$ release from membranes in which 0 (×), 49 (○), and 81% (△) of the α-BgTx sites were blocked. This membrane preparation (not the same as that in Figure 4A) had 87 ± 4% of the $^{22}Na^+$ released by 0.1 mM Carb while 1 mM PTA released only 76 ± 6% in 20 s. All data points represent the mean ± SD of triplicate determinations (no error bars are shown for ±2% or less).

on flux data characterized at these time intervals.

Agonist-Stimulated Efflux of $^{22}Na^+$: Integral Dose–Response Relations. The Carb dose–response relation based on $^{22}Na^+$ efflux measured after 20 s is shown in Figure 4A. The response defined in this manner is an integrated response and not a direct measure of the initial rate of stimulated efflux. Therefore such plots will be referred to as integral dose–response curves. Although the measured efflux depends upon the arbitrarily chosen time interval, it is possible to compare relative potency and efficacy of different agonists. The concentration of Carb associated with half-maximal response (C_{50}) is equal to 13 μM. High concentrations of two other agonists studied, AcCh and suberyldicholine, elicited the same maximal release of $^{22}Na^+$ and thus can be classified as full agonists for this response. AcCh and suberyldicholine were characterized by C_{50} values (at 20 s) of 0.7 and 0.3 μM, respectively. Phenyltrimethylammonium (PTA; Figure 4B) and hexyltrimethylammonium are partial agonists since they released 90 and 30% as much $^{22}Na^+$ as Carb. Their dose–response curves were characterized by C_{50} values of 50 and 150 μM, respectively.

Evidence for spare receptors was obtained by determining the effect of partial receptor blockade by α-BgTx on the observed dose–response relations (Figure 4). Occupancy of 47% of the receptor sites by α-BgTx increased by a factor of 4 the Carb concentration necessary to cause a half-maximal response (C_{50} = 60 μM), with only a small decrease in the amount of $^{22}Na^+$ released by high agonist concentrations. When 73% of the receptor sites were blocked with α-BgTx, the maximal response was decreased by 40% and the C_{50} was shifted further to 100 μM. The concentration dependence of the observed dose–response relations is characterized by Hill coefficients of 1.4, 1.2, and 1.1 for control, 47% blockade, and 73% blockade, respectively. For the partial agonist PTA, blockade of receptors by α-BgTx resulted in a decrease of the maximum response without any significant alteration of the observed C_{50}. Occupation of 50% of the receptor sites by α-BgTx reduced the maximal response to PTA by 75%, in contrast to the response to Carb which was reduced by only 15%.

The Carb dose–response relations observed in the absence and presence of α-BgTx, an effectively irreversible antagonist, were analyzed by the method of Furchgott & Bursztyn (1967). This analysis consists of a plot of $1/[A]$ against $1/[A']$, where [A] is the concentration of agonist giving a certain response before irreversible receptor blockade and [A′] is the concentration of agonist yielding the *same* response after receptor blockade. Furchgott & Bursztyn (1967) interpreted such a plot in terms of classical receptor theory where response is assumed to be a function of receptor occupancy and receptor occupancy follows a simply hyperbolic binding function. The concentration of drug receptor complexes ([AR]) is determined by the number of receptors (R_o), the concentration of free agonist ([A]), and an apparent dissociation constant (K_A), where $[AR] = R_o[A]/([A] + K_A)$. For [A′] to cause the same response with only a fraction (q) of functional receptors remaining, it follows that

$$\frac{R_o[A]}{[A] + K_A} = \frac{qR_o[A']}{[A'] + K_A} \quad (1)$$

Algebraic manipulation of eq 1 reveals that a plot of $1/[A]$ against $1/[A']$ is a straight line characterized by a slope equal to $1/q$ and an x intercept equal to $(q - 1)/K_A$. When the data of Figure 4A were analyzed in this manner, the plots for both 47 and 73% receptor blockades were linear, characterized by q = 0.25 and K_A = 120 μM for 47% blockade and q = 0.11 and K_A = 150 μM for 73% blockade. The interpretation of the parameter K_A depends upon the choice of the reaction mechanism determining receptor activation and will also be affected by desensitization [see Colquhoun (1973) and Discussion], but it should be a better reflection of agonist–receptor interactions than the simple C_{50} for the integral response.

It is striking that the conclusion of this analysis is that blockade of 47% of the α-toxin sites results in 25% of the receptors remaining functional even though the observed maximal response of the Carb dose–response relation was reduced only slightly due to the presence of spare receptors. In the case of the partial agonist PTA, for which the 50% α-toxin blockade resulted in a 75% reduction of the observed maximal response, the observed response is not complicated by spare receptors, and the analysis of the data by the method of Furchgott & Bursztyn (1967) also indicates that 50% α-toxin blockade results in 25% functional receptors.

Agonist-Stimulated $^{22}Na^+$ Efflux Determined by Rapid Mixing and Chemical Quenching. In order to determine the initial rate of efflux of $^{22}Na^+$ at high agonist concentration, it is necessary to measure the efflux on the subsecond time scale. In control experiments we established that *Torpedo* vesicles can be passed through two eight-jet tangential mixers at flow velocities sufficient to obtain complete mixing within 1 to 2 ms (Berger, 1964) without any loss of trapped $^{22}Na^+$.

To terminate the agonist-stimulated efflux within milliseconds, we considered the use of both competitive and noncompetitive cholinergic antagonists. In theory, high concentrations of a competitive antagonist would ensure that agonist could not rebind to receptors in the presence of the quench solution and the noncompetitive antagonist could inhibit the

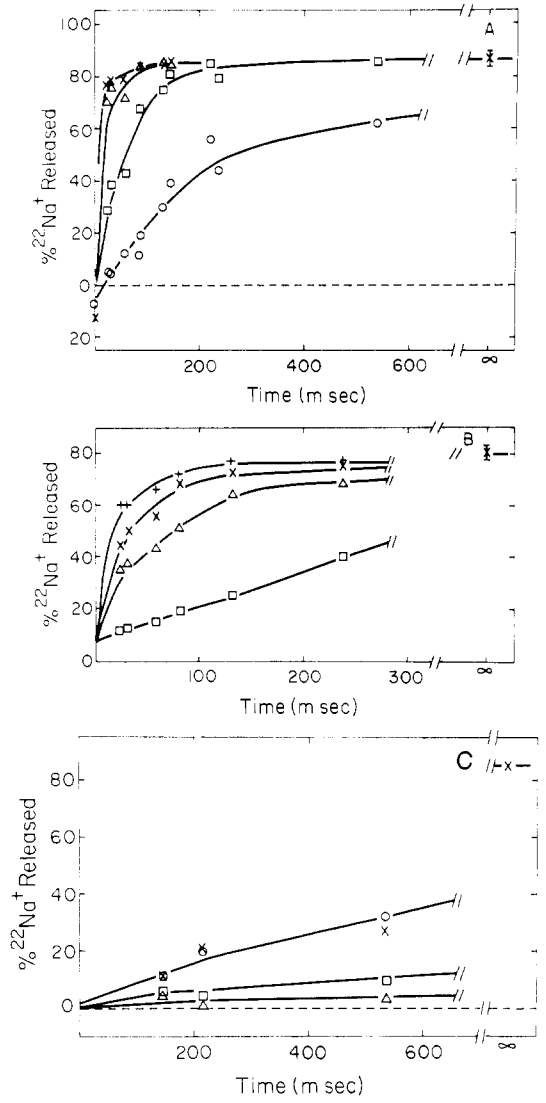

FIGURE 5: Quenched-flow determination of agonist-induced efflux of $^{22}Na^+$ from *T. nobiliana* vesicles. (A) Vesicles were equilibrated overnight with $^{22}Na^+$; external $^{22}Na^+$ and readily releasable $^{22}Na^+$ were removed as described under Materials and Methods. In the quenched-flow apparatus, equal volumes (1.2 mL) of diluted $^{22}Na^+$-loaded membrane suspensions (90 mM α-BgTx sites in TPS) and TPS containing Carb [0.2 (○), 0.6 (□), 2 (△), and 6 mM (×)] were mixed, passed through a delay tube, and then mixed with 2.4 mL of the quench solution containing 2 mM dTC and 0.2 mM meproadifen in TPS. The final reaction mixture (4.5 mL) was filtered, and the filters were washed, dried, and counted. The fraction of $^{22}Na^+$ released was determined as before. For data at zero time the Carb was added simultaneously with the quench solution, and for release at "infinite" time the quench solution was replaced with TPS and samples were filtered 10–60 min after addition of agonist. (B) Same as (A) except that α-BgTx was added to the membranes during the overnight incubation, resulting in occupancy of 70% of the receptor sites by α-BgTx. Final Carb concentrations were 0.3 (□), 1 (△), 3 (×), and 10 mM (+). (C) $^{22}Na^+$ release from untreated membranes by PTA [final concentrations: 0.01 (△), 0.1 (□), 1 (○), and 10 mM (×)].

ion transport even due to receptors still occupied by agonist. Quench solutions were tested by mixing *Torpedo* suspensions containing $^{22}Na^+$ with solutions containing 1 mM Carb plus the various antagonists. After 20 s, the following amounts of $^{22}Na^+$ were released (expressed as a percentage of that released by Carb alone): 1 mM dTC, 17%; 0.1 mM proadifen, 78%; 75 μM meproadifen, 66%; 1 mM lidocaine, 88%; 1 mM lidocaine ethyl bromide, 64%. When 1 mM dTC was used as quench, a slow stimulated efflux was detected: 3 mM Carb

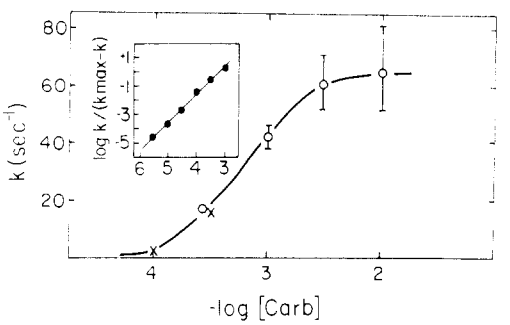

FIGURE 6: Dependence upon Carb concentration of the rate of $^{22}Na^+$ efflux from *T. nobiliana* membrane vesicles. Rate constants for $^{22}Na^+$ efflux were determined by semilogarithmic plots of the data in Figure 5. Circles (○) represent efflux from membranes pretreated with α-BgTx (data of Figure 5B), and crosses (×) indicate untreated membranes (Figure 5A). The actual observed rate constants for α-BgTx-blocked membranes are a factor of 6 lower than those presented here but are normalized to equate the response at 0.3 mM in the presence and absence of α-BgTx. Inset: Hill plot of $^{22}Na^+$ efflux rate constants. The data for 0.1 mM Carb and above are from Figure 6. The rate constants for lower Carb concentrations were determined by a nonlinear least-squares fit of the data in Figure 3 (see Materials and Methods). Units for the abscissa are the same as those for the main figure, and the line represents a linear least-squares fit of the data points (n_H = 1.96 ± 0.07).

released 50 and 85% of the $^{22}Na^+$ after 1 and 5 min, respectively. Thus, neither dTC nor the noncompetitive antagonists provided an effective quench solution when used alone. However, the combination of both 1 mM dTC and 100 μM meproadifen when mixed simultaneously with 3 mM Carb and membranes containing $^{22}Na^+$ allowed no release of $^{22}Na^+$ in 5 min.

The rapid-mix quenched-flow apparatus permits the addition of quench solutions at times as short as 24 ms after the exposure of the *Torpedo* vesicles to agonist. In the presence of 0.1 mM Carb, which causes a maximal release of $^{22}Na^+$ when measured on the slow time scale, 50% of the $^{22}Na^+$ was released in ~200 ms, while for 0.3 mM, the half-time was ~50 ms (Figure 5A). The time course of $^{22}Na^+$ efflux for these Carb concentrations is reasonably well characterized by single exponentials with rate constants 2.6 ± 0.3 and 17 ± 1 s^{-1}, respectively. Higher concentrations of Carb, however, result in the almost complete equilibration of $^{22}Na^+$ at times shorter than 24 ms. $^{22}Na^+$ efflux was measured for the same membrane suspension after blockade of 70% of the receptor sites with α-BgTx (Figure 5B) to obtain estimates of $^{22}Na^+$ efflux rates at these high concentrations. Following this treatment, the rate of release of $^{22}Na^+$ in the presence of 0.3 mM Carb was reduced by a factor of 6 relative to the unblocked membranes and the $^{22}Na^+$ efflux in the presence of higher Carb concentrations occurred during experimentally accessible times.

Responses defined as the rate constant for $^{22}Na^+$ efflux in the presence of agonists should be directly proportional to the fraction of receptors activated. Rate constants for $^{22}Na^+$ efflux at millimolar Carb concentrations in the absence of α-BgTx were calculated from the rates observed in the presence of α-BgTx. It was assumed that α-BgTx reduced the rate of efflux by the same extent for different Carb concentrations, namely, the factor of 6 observed for 0.3 mM Carb (70% block, parts A and B of Figure 5) and for 10 μM Carb (73% block, Figure 4A). The dependence of $^{22}Na^+$ efflux rate constants on Carb concentration (Figure 6) is characterized by a C_{50} of 0.6 mM. This value should be contrasted with the C_{50} = 0.013 mM for the integrated response at 20 s. On the other hand, it differs by only a factor of 4 from the C_{50} of 0.15 mM determined for the integrated response after irreversible re-

ceptor blockade. The Carb dose–response curve in Figure 6 includes only $^{22}Na^+$ efflux rate constants determined by using the rapid-mix quenched-flow technique. For concentrations of Carb of 30 μM and below, rate constants were determined by nonlinear least-squares analysis of efflux experiments performed on the 10-s time scale (Figure 3). A Hill plot of the $^{22}Na^+$ efflux rate constants determined for Carb concentrations between 3 μM and 1 mM is linear and is characterized by a slope (Hill coefficient, n_H) of 1.97 ± 0.06 (Figure 6, inset).

The maximal Carb-stimulated $^{22}Na^+$ efflux is characterized by a rate constant of 65 s^{-1}. It represents a stimulation of 5 × 10^5 over the resting efflux rate of (1.3 ± 0.4) × 10^{-4} s^{-1} (n = 18).

At Carb concentrations greater than 1 mM, semilogarithmic plots of the $^{22}Na^+$ efflux data did not extrapolate to 0% released at zero time. If the linear least-squares analyses are constrained to extrapolate to the origin, the maximal rate constant and C_{50} are 200 s^{-1} and 4 mM, respectively. However, we feel that such a constraint is not necessarily appropriate for the following reasons. (1) When the agonist is added before the quench solution, the quench may not be instantaneous. Electrophysiological studies suggest the noncompetitive antagonists do not reduce the net flux of a channel once opened (Neher & Steinbach, 1978). Therefore, the effective efflux time is underestimated. (2) Heterogeneity in the size of the vesicle population may result in nonexponential efflux kinetics on these short times. Further work with a homogeneous vesicle population (A. Jeng, unpublished observations) will be necessary to resolve the question.

In contrast to the effect of Carb, the $^{22}Na^+$ efflux in the presence of PTA is quite slow and can be readily quantified (Figure 5C). The rate of efflux in the presence of 10 mM PTA is not greater than that for 1 mM PTA and is characterized by a rate constant of 0.8 s^{-1}, only 2% of the maximal rate for Carb. The C_{50} for PTA is ~0.2 mM, a value that is within a factor of 4 of the C_{50} for the response on the 10-s time scale (0.05 mM, Figure 4B).

dTC Inhibition of Agonist-Stimulated Effluxes. The presence of high receptor densities in the *Torpedo* vesicles complicates the analysis of the mechanism of action of reversible antagonists. When the effect of dTC is measured in an integral (20 s) response assay, dTC modifies the Carb dose–response curve in a manner consistent with competitive antagonism and is characterized by an inhibition constant K_I ~ 0.5 μM [Figure 7A; see also Popot et al. (1976)]. The effect of dTC on the response to the partial agonist PTA appears noncompetitive: a concentration of 0.2 μM reduces the maximal response by 35%, while 2 μM dTC reduces it by 75% (Figure 7B). The apparent discrepancy between the effect of dTC on the full agonist Carb and that on the partial agonist PTA is most likely a result of spare receptors in the 20-s integral dose–response assay. On the millisecond time scale, 0.3 μM dTC reduces the initial rate of $^{22}Na^+$ efflux in the presence of 0.3 mM Carb by 50% (data not shown).

Discussion

Torpedo membrane vesicles provide a preparation in which both the binding of cholinergic ligands and the membrane permeability response can be determined under identical conditions. Before a relationship can be established between the receptor conformations defined by ligand binding and the functional state of the ion channel, a quantitative analysis of the permeability response must be made. The work presented here represents such an analysis.

Within the preparation of *Torpedo* postsynaptic membranes isolated by standard procedure (Cohen et al., 1972; Sobel et al., 1977), there is a vesicle population that is well sealed, characterized by half-times for $^{22}Na^+$ efflux of 60–120 min, and those vesicles provide an ideal material for the analysis of agonist dose–response relations. Exposure of the *Torpedo* vesicles to concentrations of Carb below 30 μM results in an enhanced rate of $^{22}Na^+$ efflux that can be analyzed on the multisecond time scale (Figure 3). The transient nature of the cholinergic permeability response is clearly revealed; for example, with 3 μM Carb only 60% of $^{22}Na^+$ is released before there is complete desensitization. Quantitative analyses of the efflux data to permit a characterization of both agonist-stimulated efflux rates and the kinetics and desensitization are possible (R. Neubig and J. Cohen, unpublished results).

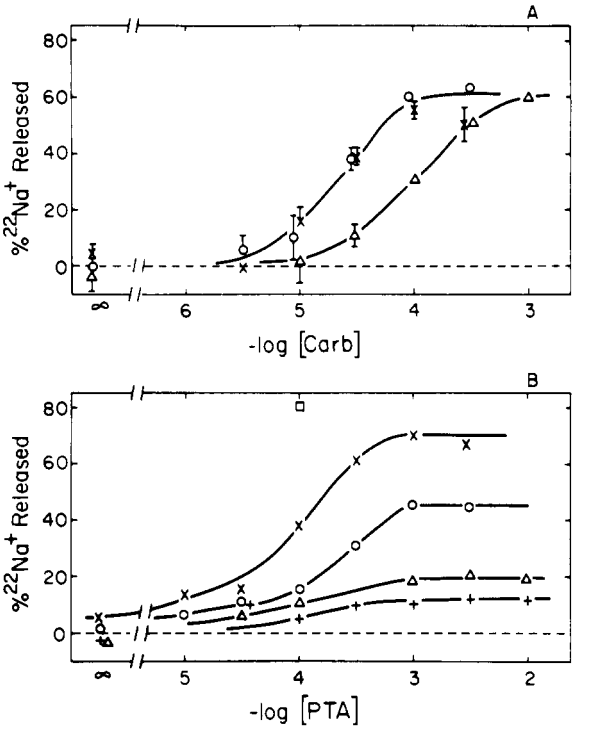

FIGURE 7: Effect of dTC on $^{22}Na^+$ release from *T. californica* membranes by Carb and PTA. Dose–response relations at 4 °C for $^{22}Na^+$ released 20 s after addition of agonist were determined as described under Materials and Methods. (A) Carb responses in the presence of dTC [0 (×), 0.2 (○), and 2 μM (△)] are the mean ± SD of triplicate determinations. (B) PTA responses in the presence of dTC [0 (×), 0.2 (○), 2 (△), and 20 μM (+)] represent duplicate determinations. The receptor site concentrations were 77 and 86 nM α-BgTx sites for (A) and (B), respectively.

To determine the initial rate of $^{22}Na^+$ efflux in the presence of high agonist concentrations, it was necessary to develop techniques to measure effluxes on the subsecond time scale. The sealed *Torpedo* vesicles are robust enough to permit mixing with agonist solutions within several milliseconds, and we identified a quench solution containing a mixture of a competitive and noncompetitive antagonist that prevents any release of $^{22}Na^+$ by 3 mM Carb when the quench solution is mixed with the membranes simultaneously with the agonist. The efflux of $^{22}Na^+$ induced by 0.1 and 0.3 mM Carb (Figure 5A) can be well characterized by a single exponential, a result that suggests the desensitization on the subsecond time scale is not significant at those concentrations. Maximal efflux rates in the presence of high Carb concentrations could not be measured directly, because in the presence of 3 mM Carb the $^{22}Na^+$ was fully released by the first observable time (24 ms). However, when 70% of the receptor sites were blocked with α-BgTx, maximal efflux rates were determined for high agonist concentrations.

When the permeability response is measured in terms of the $^{22}Na^+$ efflux rate constants, the dose–response curve for Carb (Figure 6) is characterized by a C_{50} = 600 μM, a value that is much larger than the values of 13–50 μM observed for integral (slow) responses in the *Torpedo* vesicles (Figure 4A, this work; Popot et al., 1976; Miller et al., 1978). The Hill coefficient for this response is 1.97 ± 0.06. The C_{50} values for the Carb response reported here, as well as the cooperative character of this primary response, are in good agreement with results obtained from $^{22}Na^+$ influx measurements in dissociated cultures of chick skeletal muscle ($C_{50} \simeq 800$ μM; Catterall, 1975) and from electrophysiological studies in vertebrate skeletal muscle ($C_{50} \simeq 300$ μM; Dreyer et al., 1978; Dionne et al., 1978). Hill coefficients greater than 1 were observed in earlier studies of the Carb-stimulated $^{22}Na^+$ efflux from *Torpedo* vesicles. However, in those studies neither the C_{50} values nor the observed Hill coefficients reflect receptor activation in a direct manner because of the existence of spare receptors. Clark (1937) noted many years ago that if a full response results from activation of a small fraction of the available receptors, dose–response relations will appear cooperative in the absence of a true cooperative response.

The maximal rate of $^{22}Na^+$ efflux observed for Carb, k_{max} = 65 s^{-1}, represents an enhancement of 5 × 10^5 over the unstimulated efflux rate. In contrast, for chick skeletal muscle the Carb-stimulated efflux represented an enhancement of about 20-fold (Catterall, 1975) and for *Electrophorus* vesicles saturating agonist concentrations increased the efflux rate by about 50-fold [Hess & Andrews, 1977; but see also Hess et al. (1978)].[2] The extraordinary enhancement of $^{22}Na^+$ efflux from the *Torpedo* vesicles by agonist reflects the high density of receptors in the vesicles, and it permits the conclusion that less than 2 × 10^{-4}% of the ion channels are conducting in the absence of agonist!

Functional studies of the nicotinic AcCh receptor indicate the existence of three conformations of differing affinity for agonist and differing functional states of the channel: R_c, the low-affinity conformation associated with closed channels; R_o, the open-channel conformation; R_d, the high-affinity desensitized conformation. We present a three-state model (Figure 8A) to describe AcCh receptor function. This model includes no open channels in the absence of agonist (see above) and 2 agonist binding sites/receptor, in accord with the cooperativity of responses (n_H = 1.97 ± 0.06). The isomerization between A_2R_c and A_2R_o must occur on the millisecond time scale since channel opening and closing at the vertebrate neuromuscular junction and in *Torpedo* vesicles (this report) occur in milliseconds.

A major goal of this research was to allow a direct comparison between agonist binding and the associated permeability response. Analysis of the kinetics of agonist binding (Heidmann & Changeux, 1979; Cohen & Boyd, 1979) revealed a transient low-affinity binding thought to be related to agonist equilibrating with R_c and R_o. In addition, direct evidence was provided for a fraction of the receptors preexisting in the high-affinity conformation (R_d) predominant at equilibrium. The kinetics of flux desensitization in the presence of low agonist concentrations (as in Figure 3) are the same as the kinetics of the conformational isomerization from low- to high-affinity binding of [^{3}H]Carb and [^{3}H]AcCh [R. Neubig, N. Boyd, and J. Cohen, unpublished observation; see also Sine & Taylor (1979)]. This suggests that the high-affinity receptor conformation is truly desensitized.

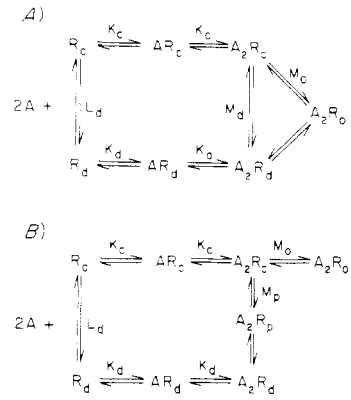

FIGURE 8: Nomenclature for three-state (A) and four-state (B) models. R_c represents the receptor conformation binding agonist with low affinity that preexists in the absence of cholinergic ligand and is associated with closed channels; R_d is the preexisting high-affinity (desensitized) conformation; R_o represents the receptor conformation associated with activated ion channels. In the four-state model, R_p is a conformation populated only transiently that is either completely inactive or transporting ions inefficiently. K_c and K_d are microscopic dissociation constants for agonist binding to the closed and desensitized receptor conformations. L_d and M_x (x = o, d, and p) are receptor isomerization constants where $L_d = [R_c]/[R_d]$ and $M_x = [A_2R_x]/[A_2R_c]$. In the four-state model, A_2R_p is the new receptor state postulated to account for the transient low-affinity binding of agonists (see text). From the analyses of the kinetics of binding of agonists, data have been obtained which define L_d, K_d, and their associated rate constants as well as an apparent equilibrium constant and rate constants related to the low-affinity binding of agonists. As discussed in the text, we believe that the flux dose–response relations reported here reflect K_c and M_o while the transient low-affinity binding reflects K_c and M_p.

The apparent K_D values for the transient, low-affinity binding of a fluorescent cholinergic compound (Heidmann & Changeux, 1979) and [^{3}H]AcCh and [^{3}H]Carb (Cohen & Boyd, 1979; N. D. Boyd and J. B. Cohen, unpublished results) are 1, 1, and 20 μM, respectively. The good correlation between these values and the C_{50} values for the $^{22}Na^+$ efflux in a slow assay raised the possibility that the low-affinity binding is associated with channel activation. However, the C_{50} = 600 μM characterizing the initial rate of Carb-stimulated $^{22}Na^+$ efflux reported here is 30-fold higher than the C_{50} for the low-affinity binding of [^{3}H]Carb. Given the rapid equilibrium of A_2R_c and A_2R_o, the three-state model predicts that the largest difference expected corresponds to C_{50}(response)/C_{50}(low-affinity binding) = 2.4 (see Appendix). Furthermore, the rate constants for the appearance of low-affinity binding are considerably slower than those associated with channel opening and closing (Heidmann & Changeux, 1979; Cohen & Boyd, 1979; N. D. Boyd and J. B. Cohen, unpublished results). These discrepancies lead to the conclusion that the three-state model cannot account for both agonist binding and response and that the observed transient low-affinity binding is associated with a previously unidentified state of the nicotinic receptor–channel complex.

A modification of the three-state model that can account for both the kinetics of ligand binding and the C_{50} for $^{22}Na^+$ efflux is summarized in Figure 8B. The significant feature of the model is the inclusion of a fourth state, R_p, that is associated with the observed low-affinity binding (A_2R_p). This model makes several testable predictions. While the A_2R_p state cannot represent a conformation transporting ions with high efficiency, we cannot distinguish between its being completely

[2] As this manuscript was nearing completion, a report was published (Hess et al., 1979) describing the use of a quench-flow technique to measure agonist-stimulated $^{22}Na^+$ influx in *Electrophorus* vesicles. That report describes desensitization in the eel system but does not consider agonist dose–response relations or maximal transport rates.

inactive or its being partially active (say 1% of the A_2R_o state). In either case, there will be two phases of desensitization associated with the appearance of A_2R_p and A_2R_d, respectively. The model also allows us to predict experimental conditions under which the biphasic desensitization rate should be observable. As the model is presented in Figure 8B in which it is assumed that monoliganded AR_p does not exist, the two phases of desensitization can be observed only at high agonist concentrations; the existence of the A_2R_p state decreases the maximal response while the responses at low agonist concentrations are unaffected. If AR_p is significant, two phases of densitization should be observed at all agonist concentrations. Finally, this model predicts that the steady-state response (after equilibration of A_nR_c, A_2R_o, and A_2R_p but before appreciable concentrations of A_nR_d appear) will be less than the response predicted from single channel events. As discussed below, this has been seen in all measurements of steady-state responses.

In addition to providing new information about the concentration dependence of channel activation, the studies reported here provide new information about the ion transport efficiency of the membrane-bound *Torpedo* receptor. The observed k_{max} = 65 s^{-1} is equivalent to a transport of 3.5 Na^+/(α-BgTx site ms). This value is 8% of the maximal rates reported by Catterall (1975) for the Carb-stimulated $^{22}Na^+$ influx in chicken skeletal muscle at 2 °C, and in that system the observed k_{max} is ~10% of the rate expected from the single channel conductance (Catterall, 1975; T. Gibbs, personal communication). The maximal steady-state conductance per α-BgTx site observed with Carb in the isolated *Electrophorus* electroplaque is also ~1% of the single channel conductance (Lester et al., 1975). Since our calculation assumes that all the α-BgTx sites are involved in ion transport, the calculated transport number is probably an underestimate. In our experiments, the internal volume of the well sealed vesicles is only half the total internal volume and there may be a significant fraction of α-BgTx sites in unsealed vesicles. Clearly, fractionation of the *Torpedo* membrane suspension to separate sealed from unsealed vesicles will permit a more realistic assessment of the transport efficiency of the receptor in its postsynaptic membrane. However, it appears reasonable to conclude at this time that the efficiency of agonist-mediated ion transport in the isolated *Torpedo* vesicles is within the range observed for intact cells.

Analysis of the initial rates of $^{22}Na^+$ efflux stimulated by PTA reveals a significant difference between the action of that agonist and the action of Carb. Clearly, PTA is a partial agonist and the difference between PTA and Carb is much more striking when expressed as rate constants for $^{22}Na^+$ release than as the maximal amount of $^{22}Na^+$ released in a slow assay (Figure 5C). The maximal rate for PTA, k = 0.8 s^{-1}, was only 2% of the maximal Carb rate. Further studies will be necessary to determine the molecular basis of the low transport rates observed for PTA.

The studies presented here permit a comparison of the agonist dose–response relations obtained from a response proportional to channel activation with that obtainable from integral responses. In order to correct the integral responses for the presence of spare receptors, we used the method of Furchgott (1966) where the responses to agonist before and after partial blockade of receptors with an irreversible antagonist are used to estimate the true K_A for receptor activation. The K_A values estimated by this method for Carb and PTA (150 and 50 μM, respectively) are a factor of 4 lower than those determined from the initial rate of $^{22}Na^+$ efflux. Since the C_{50} for Carb obtained in the standard integral assay is ~20 μM, the result of the Furchgott analysis provides a better estimate of the true K_A. It is striking that the dose–response curve measured at 20 s in the presence of α-BgTx is characterized by a Hill coefficient n_H of 1.1, in disagreement with the n_H = 2 observed for the initial rate dose–response. The disagreements between the results of the Furchgott analysis and the initial rate data for both C_{50} and Hill coefficient reflect in part the fact that desensitization occurs on the 20-s time scale in the presence of Carb and PTA, while for the Furchgott analysis to be rigorously correct there must be no desensitization.

Table I: Comparison of Calculated and Observed Response (q) after Occupation of a Fraction (P_B) of Receptor Sites by α-BgTx[a]

		q for P_B				
n	i	0	0.47	0.70	0.73	0.80
1	1	1	0.53	0.30	0.27	0.20
2	1	1	0.28	0.09	0.07	0.04
4	1	1	0.08	0.008	0.005	0.002
4	2	1	0.36	0.08	0.06	0.03
obsd for Carb		1	0.25[b]	0.16[c]	0.11[b]	
obsd for PTA		1	0.27[b]			0.12[b]

[a] The fraction of the response remaining (q) was calculated by assuming that i or more α-BgTx bound to a receptor containing n sites would completely inactivate that receptor, while a receptor with less than i α-BgTx bound would not be affected. The probability of a receptor binding m α-BgTx molecules is $\binom{n}{m} P_B^m (1 - P_B)^{n-m}$ where P_B is the total fraction of α-BgTx sites occupied. [b] Determined by Furchgott analysis (Furchgott & Bursztyn, 1967) of dose–response curves in Figure 4. [c] Determined from the ratio of initial rate of $^{22}Na^+$ efflux in the presence of 0.3 mM Carb with and without 70% of the α-BgTx sites blocked (parts A and B of Figure 5).

One of the parameters derived in the Furchgott analysis is the fraction of the response remaining (q), and we have also determined the reduction by α-BgTx of the initial rate of $^{22}Na^+$ efflux for 0.3 mM Carb. Since we have determined directly the fraction (P_B) of receptor sites occupied by α-BgTx, it is possible to use this information to determine the number of α-BgTx sites per functional receptor unit. It is known that the *Torpedo* receptor exists in detergent solution as a monomer (M_r 250 000; two α-BgTx sites) and as a dimer (M_r 500 000; four α-BgTx sites) (Reynolds & Karlin, 1978) and that the number of AcCh binding sites is equal to the number of α-BgTx sites (Neubig & Cohen, 1979). Thus, it is likely that the number of AcCh sites per functional receptor is less than or equal to four. We have calculated the expected response remaining (q) as a function of P_B by assuming that the binding of i or more α-BgTx molecules to a functional receptor containing n sites completely inhibits the response. The probability of a receptor with n sites having m α-BgTx molecules bound is determined by the fractional occupancy of sites (P_B) and is equal to $\binom{n}{m} P_B^m (1 - P_B)^{n-m}$ if α-BgTx binds independently to each site. In Table I is presented expected and observed values q as a function of P_B for functional receptor units containing n = 1, 2, or 4 sites. Both the Carb and PTA data agree reasonably well with the case of a single α-BgTx molecule completely inhibiting a functional receptor with n = 2. At large extents of blockade, however, there is more response remaining than would be expected. This could be due to partial activity of a receptor occupied by one α-BgTx or to displacement of α-BgTx by high agonist concentrations. These observations, in conjunction with the Hill coefficient of 1.97 ± 0.06 for Carb-induced $^{22}Na^+$ efflux, suggest that the functional unit of the AcCh receptor contains two sites and that both must be occupied by agonist to elicit a significant response.

While apparent dose–response relations based on integral responses (the 20-s assay in this report) give erroneous estimates of agonist–receptor interactions in the presence of spare receptors, classical pharamacological theory indicates that it should be possible to determine true affinities for reversible antagonists even in the presence of spare receptors. Recent studies of the direct binding of [^{3}H]dTC to *Torpedo* membranes have established that the total number of dTC binding sites is equal to that of AcCh or α-BgTx but that half the sites are characterized by a dissociation constant K_{D1} of 10–30 nM and half by a K_{D2} of 7 μM (Neubig & Cohen, 1979). However, in the $^{22}Na^+$ flux assay, we observed (Figure 7A) that the effects of dTC on the Carb response measured at 20 s are consistent with competitive antagonism characterized by $K_I \sim 0.5$ μM [see also Popot et al. (1976)]. When PTA was the agonist (Figure 7B), the dTC appeared noncompetitive. These apparently inconsistent results can be explained by two observations. First, [^{3}H]dTC dissociates from its high-affinity binding site with a half-time at 4 °C of 10 s (R. Neubig, unpublished results). In the absence of spare receptors, this slow dissociation of dTC will result in a depression of the maximal response in a 20-s assay. Second, dTC stabilizes the high-affinity (desensitized) conformation of the *Torpedo* nicotinic receptor (Cohen, 1978; Krodel et al., 1979) and desensitization should also contribute to a depression of the maximal response. In the 20-s flux assay, the presence of spare receptors for Carb will mask this depression of the maximal response and the dose–response curve will appear shifted to the right. Further study will be necessary to define the exact mechanisms for dTC's inhibition of responses by different agonists.

The studies reported here serve as an introduction to the quantitative analysis of agonist and antagonist mechanisms now possible with the use of rapid-mixing and quenched-flow techniques. Analysis on the millisecond time scale of the functional state of the membrane-bound *Torpedo* receptor will help elucidate the relation between ligand binding and receptor function.

Acknowledgments

We thank Bernard Corrow and Arthur Larson for their assistance in the construction of the quenched-flow apparatus and Dr. D. Auld for suggestions concerning its calibration. We also thank Drs. P. Boquet, A. Menez, J. L. Morgat, and P. Fromageot for a gift of the [^{3}H]-α-toxin of *N. nigricollis*.

Appendix

Comparison of Concentration Dependence of Receptor Occupancy and Channel Activation in a Three-State Model of Receptor Function. The discrepancy between the C_{50} for receptor activation and that for transient low-affinity binding is an important observation for ruling out the three-state model (Figure 8A). Here we examine the C_{50} values predicted for these processes by the three-state model. Since the increase in A_nR_d (the high-affinity state) is slow compared to receptor activation and the appearance of transient low-affinity binding (Cohen & Boyd, 1979; N. D. Boyd and J. B. Cohen, unpublished results), we neglect the A_nR_d states (n = 0, 1, and 2), leaving the activation model:

$$2A + R_c \overset{K_c}{\rightleftharpoons} AR_c \overset{K_c}{\rightleftharpoons} A_2R_c \overset{M_o}{\rightleftharpoons} A_2R_o$$

The agonist A binds independently to two sites on the receptor with microscopic dissociation constant K_c. M_o is equal to $[A_2R_o]/[A_2R_c]$, and the normalized agonist concentration $\alpha = [A]/K_c$. The fraction of receptors in the open conformation is

$$\bar{R} = \frac{M_o\alpha^2}{1 + 2\alpha + (M_o + 1)\alpha^2}$$

and the fractional binding site occupancy is

$$\bar{Y} = \frac{\alpha + (M_o + 1)\alpha^2}{1 + 2\alpha + (M_o + 1)\alpha^2}$$

Thus, the maximal response attainable is $M_o/(M_o + 1)$, and the half-maximal response occurs for a concentration of A equivalent to

$$\alpha_{0.5}{}^* = \frac{1 + (M_o + 2)^{1/2}}{M_o + 1}$$

The normalized agonist concentration for half-maximal binding is

$$\alpha_{0.5} = \frac{1}{(M_o + 1)^{1/2}}$$

The ratio of the concentration producing the half-maximal response to that associated with half-maximal binding is

$$\frac{\alpha_{0.5}{}^*}{\alpha_{0.5}} = \frac{1 + (M_o + 2)^{1/2}}{(M_o + 1)^{1/2}}$$

which ranges from 1 for large values of M_o to $1 + 2^{1/2}$ for small M_o values. Thus, the three-state model *cannot* account for the 30-fold discrepancy between binding and response.

References

Andreasen, T. J., & McNamee, M. G. (1977) *Biochem. Biophys. Res. Commun. 79*, 958–965.

Bard, Y. (1967) Nonlinear Parameter Estimation and Programming Program 360D 13.6.003 IBM, Hawthorne, New York.

Barman, T. E., & Gutfreund, H. (1964) in *Rapid Mixing and Sampling Techniques in Biochemistry* (Chance, B., Eisenhardt, R. H., Gibson, Q. H., & Lonberg-Holm, K. K., Eds.) pp 339–344, Academic Press, New York.

Berger, R. L. (1964) in *Rapid Mixing and Sampling Techniques in Biochemistry* (Chance, B., Eisenhardt, R. H., Gibson, Q. H., & Lonberg-Holm, K. K., Eds.) pp 33–38, Academic Press, New York.

Bernhardt, J., & Neumann, E. (1978) *Proc. Natl. Acad. Sci. U.S.A. 75*, 3756–3760.

Cartaud, J., Benedetti, L., Cohen, J. B., Meunier, J. C., & Changeux, J. P. (1973) *FEBS Lett. 33*, 109–113.

Catterall, W. A. (1975) *J. Biol. Chem. 250*, 1776–1781.

Chance, B. (1974) *Tech. Chem. (N.Y.) 6*, 5–62.

Clark, A. J. (1937) *Hand. Exp. Pharmakol. 4*, 1–228.

Cohen, J. B. (1978) in *Molecular Specialization and Symmetry in Membrane Function* (Solomon, A. K., & Karnovsky, M., Eds.) pp 99–128, Harvard University Press, Cambridge, MA.

Cohen, J. B., & Boyd, N. D. (1979) in *Catalysis in Chemistry & Biochemistry* (Pullman, B., Ed.) pp 293–304, D. Reidel, Dordrecht, Netherlands.

Cohen, J. B., Weber, M., Huchet, M., & Changeux, J. P. (1972) *FEBS Lett. 26*, 43–47.

Colquhoun, D. (1973) in *Drug Receptors* (Rang, H. P., Ed.) pp 149–182, Macmillan, London.

Dionne, V. E., Steinbach, J. H., & Stevens, C. F. (1978) *J. Physiol. (London) 281*, 421–444.

Dreyer, F., Peper, K., & Sterz, R. (1978) *J. Physiol. (London) 281*, 395–419.

Eldefrawi, M. E., Eldefrawi, A. T., Mansour, N. A., Daly, J. W., Witkop, B., & Albuquerque, E. X. (1978) *Biochemistry 17*, 5474–5483.
Elliott, J., & Raftery, M. A. (1979) *Biochemistry 18*, 1868–1874.
Froehlich, J. P., & Taylor, E. W. (1976) *J. Biol. Chem. 251*, 2307–2315.
Furchgott, R. F. (1966) *Adv. Drug. Res. 3*, 21–55.
Furchgott, R. F., & Bursztyn, P. (1967) *Ann. N.Y. Acad. Sci. 144*, 882–899.
Gage, P. W. (1976) *Physiol. Rev. 56*, 177–247.
Gibson, Q. H., & Milnes, L. (1964) *Biochem. J. 91*, 161–171.
Heidmann, T., & Changeux, J. P. (1978) *Annu. Rev. Biochem. 47*, 371–411.
Heidmann, T., & Changeux, J. P. (1979) *Eur. J. Biochem. 94*, 255–279.
Hess, G. P., & Andrews, J. P. (1977) *Proc. Natl. Acad. Sci. U.S.A. 74*, 482–486.
Hess, G. P., Lipowitz, S., & Struve, G. F. (1978) *Proc. Natl. Acad. Sci. U.S.A. 75*, 1703–1707.
Hess, G. P., Cash, D. J., & Aoshima, H. (1979) *Nature (London) 282*, 329–331.
Holmquist, B., & Bruice, T. C. (1969) *J. Am. Chem. Soc. 91*, 2982–2985.
Kasai, M., & Changeux, J. P. (1971) *J. Membr. Biol. 6*, 1–80.
Katz, B., & Thesleff, S. (1957) *J. Physiol. (London) 138*, 63–80.
Krodel, E. K., Beckman, R. A., & Cohen, J. B. (1979) *Mol. Pharmacol. 15*, 294–312.
Lester, H. A., Changeux, J. P., & Sheridan, R. E. (1975) *J. Gen. Physiol. 65*, 797–816.
Lowry, O., Rosebrough, N., Farr, A., & Randall, R. J. (1951) *J. Biol. Chem. 193*, 265–275.
Miller, D. L., Moore, H.-P. H., Hartig, P. R., & Raftery, M. A. (1978) *Biochem. Biophys. Res. Commun. 85*, 632–640.
Neher, E., & Steinbach, J. H. (1978) *J. Physiol. (London) 277*, 153–176.
Neubig, R. R., & Cohen, J. B. (1979) *Biochemistry 18*, 5464–5475.
Neubig, R. R., Krodel, E. K., Boyd, N. D., & Cohen, J. B. (1979) *Proc. Natl. Acad. Sci. U.S.A. 76*, 690–694.
Popot, J. L., Sugiyama, H., & Changeux, J. P. (1976) *J. Mol. Biol. 106*, 469–483.
Quast, U., Schimerlik, M., Lee, T., Witzemann, V., Blanchard, S., & Raftery, M. A. (1978) *Biochemistry 17*, 2405–2414.
Reynolds, J. A., & Karlin, A. (1978) *Biochemistry 17*, 2035–2038.
Sine, S., & Taylor, P. (1979) *J. Biol. Chem. 254*, 3315–3325.
Sobel, A., Weber, M., & Changeux, J. P. (1977) *Eur. J. Biochem. 80*, 215–224.
Stephenson, R. P. (1956) *Br. J. Pharmacol. Chemother. 11*, 379–393.
Sugiyama, H., Popot, J. L., & Changeux, J. P. (1976) *J. Mol. Biol. 106*, 485–496.
Sumida, M., Wang, T., Mandel, F., Froehlich, J. P., & Schwartz, A. (1978) *J. Biol. Chem. 253*, 8772–8777.
Weiland, G., Georgia, B., Lappi, S., Chignell, C. F., & Taylor, P. (1977) *J. Biol. Chem. 252*, 7648–7656.

Dynamical Structure of Phosphatidylcholine Molecules in Single Bilayer Vesicles Observed by Nitrogen-14 Nuclear Magnetic Resonance†

Keiko Koga and Yoko Kanazawa*

ABSTRACT: A ^{14}N nuclear magnetic resonance (NMR) study of lecithins, 24–65 °C for dipalmitoylphosphatidylcholine (DPPC) and 20–50 °C for egg yolk phosphatidylcholine (EPC), in single bilayer vesicles prepared by an ultrasonic method is reported. Choline ^{14}N signals are found to be Lorentzian in these systems of definite molecular arrangement because of the smallness of the quadrupole coupling constant. This is due to the high symmetry around the trimethylammonium type nucleus and to the low ordering compared with thermotropic liquid crystals. An analysis of relaxation times T_1 and T_2 gives the following results. (1) The activation energies for the rapid local motion of C_β–N bonds are 36 and 31 kJ·mol^{-1} for DPPC and EPC, respectively. These are higher than that of a C_α–D bond, indicating that the $-N^+(CH_3)_3$ group is bound in the polar surface. (2) The vesicle radius seems to decrease toward higher temperatures, just below the start of the phase transition. (3) The lateral diffusion coefficient of the constituent lipid is obtained with the help of the Stokes radius. The ^{14}N NMR technique has the essential advantage of applicability without modification of the system.

The physical properties of model membrane systems consisting mainly of phospholipids have been investigated by various methods. The significance of spectroscopic work is evident for the dynamical study of membrane phenomena at the molecular level. *N*-Oxide spin-label electron spin resonance (ESR)[1] has been a powerful technique to detect various physical properties (see, e.g., Wu & McConnell, 1975; Ito & Ohnishi, 1975). The fluorescent probe method has also been used extensively to observe the fluidity and phase transitions of the membranes (see, e.g., Lentz et al., 1976; Wu et al., 1977). These techniques necessarily include the use of probes, which are either modified lipids or foreign molecules, giving more or less modification of the system.

For studies of the hydrophilic part of the membrane and of perturbations of the system such as the effects of drugs, the

† From the Faculty of Pharmaceutical Sciences, Kyushu University, Maidashi, Higashi-ku, Fukuoka 812, Japan. *Received August 17, 1979.*

[1] Abbreviations used: ESR, electron spin resonance; NMR, nuclear magnetic resonance; FT, Fourier transform; DPPC, 1,2-dipalmitoyl-3-*sn*-phosphatidylcholine; DMPC, 1,2-dimyristoyl-3-*sn*-phosphatidylcholine; EPC, egg yolk phosphatidylcholine; CTAB, *n*-hexadecyltrimethylammonium bromide; HTAB, *n*-hexyltrimethylammonium bromide.

0006-2960/80/0419-2779$01.00/0